Atmospheric Corrosion of Engineering Materials at Two Exposure Sites in Chennai—A Comparative Study

M. Natesan,[‡,] S. Palraj,[*] G. Venkatachari,[*] and N. Palaniswamy[*]*

ABSTRACT

Atmospheric corrosion of engineering materials such as mild steel, galvanized iron, zinc, and aluminum at marine and industrial environments in Chennai has been studied. Monthly and yearly corrosion rates were determined using the weight-loss method. The average levels of pollutants, viz., salinity and sulfur dioxide (SO_2), in both atmospheres have been measured. The results of five-year corrosion exposure tests agree well with the kinetic equation of the form $V_{corr} = kt^n$, where k and V_{corr} are the weight losses after 1 and "t" years of the exposure, respectively, and n is a constant. Based on the n value, the corrosion mechanisms of these metals have been predicted. The corrosion products of the materials were analyzed using x-ray diffraction (XRD) and scanning electron microscopy (SEM) techniques.

KEY WORDS: atmospheric corrosion, Chennai, corrosion rate, industrial, marine, metals, statistical approach

INTRODUCTION

The damage to metals caused by corrosion in various environments has been studied.[1-6] The corrosion behavior of metal is mainly influenced by climatic and pollution factors in the surrounding atmosphere. Corrosion loss of iron, copper, zinc,[7] and aluminum was found to be dependent on relative humidity, the time of wetness, and the amount of chloride and sulfur dioxide (SO_2) present in the atmosphere. High corrosion rates in industrialized areas have been encountered due to high SO_2 concentrations. Chloride content in the marine area has been shown to have a substantial effect on the corrosion of iron,[8-9] zinc,[10] copper,[11] and aluminum.[12] The high resistance of zinc and copper against atmospheric corrosion compared to iron was attributed to the formation of protective corrosion products[13] in which the aggressive ions are captured and inactivated. The corrosion resistance behavior of aluminum was explained by the formation of amorphous hydroxides immobilizing aggressive ions.[14] However, the field corrosion mechanisms have not been fully understood so far, since most of the time the quantity of metal released from the surface by rainfall or wind velocity has not been evaluated. Consequently, field corrosion mechanisms may be considered to be a major contributor to the overall costs of corrosion, which has been estimated to be in the range of 4% to 5% of the gross national product (GNP) for several countries.[15] Atmospheric corrosion is the major contributor to this cost. Updating a corrosion map of India is a project in the field of atmospheric corrosion. The details of this project and the results obtained from the 41 field exposure stations have been published.[16-20]

The goal of the Indian program is to collect the corrosiveness data from various locations in India for preparing a new corrosiveness map. This paper presents corrosiveness data obtained from monthly and 1-year to 5-year atmospheric exposures of widely used engineering materials such as mild steel (MS), galvanized iron (GI), zinc, and aluminum in marine and industrial exposure sites. The effects of climate

Submitted for publication September 2005; in revised form, April 2006.

‡ Corresponding author. E-mail: mnatesan@rediffmail.com.

* Corrosion Science and Engineering Division, Central Electrochemical Research Institute, Karaikudi – 630 006 T.N. India.

TABLE 1
Chemical Composition of Test Materials (wt%)

Metal	C	Mn	Si	P	S	Cr	Mo	Ni	Al	Cu	Sn	Mg	Cd	Pb	Zn	Fe
MS	0.01	0.196	0.007	0.009	0.014	0.043	0.015	0.013	—	—	—	—	—	—	—	Bal.
Zn	—	—	—	—	—	—	—	—	0.001	0.007	0.001	—	0.0045	0.012	Bal.	0.00145
GI[(A)]	—	—	—	—	—	—	—	—	0.002	—	<0.01	<0.01	—	0.10	Bal.	—
Al	—	0.015	0.32	—	—	<0.005	—	—	Bal.	0.015	—	0.13	—	—	0.003	0.51

[(A)] GI (in Zn coating).

and pollutants on the degradation of materials are discussed. Statistical analysis was carried out and the corrosion mechanism has been predicted.

EXPERIMENTAL PROCEDURES

The exposure test was performed at the Chennai (marine) and Manali (industrial) sites situated in southern India. The Chennai marine site is 14 km from the Manali industrial site. The marine site is situated at a latitude of 13°06' North and a longitude of 80°18' East. It is about 150 m away from the Bay of Bengal coast and situated near the port of Chennai. The port handles coal, crude oil, iron ore, and other industrial products; therefore, a lot of dust particles are found deposited on the metal surface. The major pollutant in the area is chloride. The exposure studies were carried out from April 1999 to May 2004 for 5 years. The widely used engineering materials such as MS, GI, zinc, and aluminum of size 100 by 150 mm and thickness of 2.5 mm were exposed for 1 year to 2 years and 4-mm-thick materials were exposed for more than 2 years. The reason for this was to avoid the latter samples breaking during the time of exposure. The chemical composition of each metal is given in Table 1. They were polished with a 120 emery wheel, degreased with trichloroethylene, dried, and weighed to an accuracy of 0.1 mg prior to the exposure. Then the specimens were mounted on the exposure stands at an angle of 45° from the horizontal and both sides were exposed. In order to identify the exposed specimens, stamped code numbers were used. The exposure stands were located in open atmosphere carefully avoiding shadows of trees, buildings, or structures. Atmospheric exposure studies were carried out according to the ISO/DIS 8565 norm[21] and IS 5555-1970.[22] The corrosion products were removed using the respective cleaning solutions.[23]

Triplicate specimens of each metal were collected at each month and 1-year intervals from these exposure sites for weight-loss determination and surface analysis. The specimens were derusted, dried, and reweighed, and the average corrosion rate was determined from the weight loss as described elsewhere.[21] The corrosion rate of each metal was determined by considering the total affected area, faces to the sky and to the ground, metal density and exposure time, and corrosion rates expressed in μm/y. Guidelines from an Indian standard,[22] the International Organization for Standardization (ISO),[21] and ASTM International[24] were used for the exposure and cleaning procedures required before exposure and for cleaning and evaluation after the exposure. The climatic parameters such as temperature, relative humidity (RH), and rainfall were obtained from the nearest Chennai meteorological station. The monthly and yearly average values of these parameters were calculated. Pollution due to SO_2 and airborne salinity represented by chloride were evaluated continuously every month for the period of 1 year by the deposition methods (by lead peroxide [PbO_2] and wet candle methods, respectively).[22,25] SO_2 of the atmosphere absorbed by the PbO_2 was transformed into lead sulfate ($PbSO_4$), which was then analyzed using the gravimetric method. The amount of chloride absorbed by capillary action by the wet candle was determined using the titration method. The environmental characteristics of the exposure sites were classified using ISO 9223.[26]

To determine the mathematical model, the data for the 5-year exposure was used. First, the potential law:[27]

$$V_{corr} = kt^n \quad (1)$$

where V_{corr} is the weight loss expressed in mm, k and n are constants, and t is time of exposure in days. In a later phase, the following model, which was more accurate than the potential law, was applied:[28-30]

$$V_{corr} = kt^n \times 10^{[a(SO2)+b(Cl)+c(W)]} \quad (2)$$

where V_{corr} is the corrosion rate measured in μm; k, a, b, and c are constants (SO_2) as the concentration of SO_2 in mg/(m^2-day); (Cl^-) is the concentration of chloride in mg/(m^2-day); t is time of exposure in days; and W is the total rainfall (mm). After the specified exposure period, the metal panels were removed from the exposure stand to determine weight loss and surface analysis (x-ray diffraction [XRD] and scanning electron microscopy [SEM]). The corrosion product analyses were carried out using XRD techniques with JEOL-JDX-8030[†] computer-controlled equipment, and the corroded surfaces were investigated using the SEM model HITACHI S-3000H[†]. The XRD patterns were obtained between 10° and 70° two theta. The

[†] Trade name.

TABLE 2

Average Monthly Values of Environmental and Pollution Factors in Marine and Industrial Sites in Chennai

Environment	Period	Temperature (°C)		RH (%)		Rainfall (mm)	SO_2 mg/(m²-day)	Chloride mg/(m²-day)
		Maximum	Mininum	Maximum	Minimum			
Marine	April 1999	38.0	22.0	91	58	6	26	321
	May	38.5	25.0	92	67	26	18	318
	June	38.0	27.0	94	69	47	15	300
	July	36.0	25.0	91	62	91.0	14	298
	August	35.0	30.0	96	58	116.0	17	301
	September	34.0	25.0	93	54	119.0	16	294
	October	33.0	24.0	92	59	306.0	19	308
	November	30.0	22.0	94	63	355.0	18	382
	December	34.0	20.5	98	61	138.0	19	301
	January 2000	30.0	19.5	92	55	36.0	16	294
	February	34.0	20.0	97	59	10.0	19	302
	March	33.0	22.0	95	45	7.0	20	315
Industrial	April 1999	37.0	20	93	57	6	24.5	78.5
	May	39	25	90	62	26	23.1	74.3
	June	36	28	95	71	43	26.2	72.1
	July	34	26	91	60	86	26.5	65.8
	August	36	29	90	58	123	25.0	68.3
	September	35	26	84	59	117	24.8	72.0
	October	33	24	90	56	312	23.5	65.4
	November	30	19	88	61	309	27.0	61.6
	December	33	22	95	56	142	23.2	58.1
	January 2000	31	20	91	57	45	22.0	72
	February	34	21	96	61	8.6	29.0	74
	March	34	23	83	51	5.0	22.0	72

TABLE 3

Average Yearly Values of Environmental and Pollution Data of Marine and Industrial Exposure Sites in Chennai

Period (Year)	Environment	Meterological				Rainfall Maximum (mm)	SO_2 (mg/m²-day)	Chloride (mg/m²-day)
		Mean Temperature (°C)		Mean RH (%)				
		Maximum	Minimum	Maximum	Minimum			
1	Marine	39	20	98	59	355	18	304.6
2		38	20	98	59	320	20	302.1
3		38	21	98	58	390	24	300.8
4		37	22	97	58	405	22	304.2
5		38	21	99	59	420	19	303.6
1	Industrial	39	19	98	61	309	25	75.2
2		40	22	85	60	300	28	74.9
3		39	18	86	62	295	26	74.6
4		40	19	88	63	301	24	78.8
5		38	18	87	61	310	27	74.5

phases present were identified using the PCPDFWIN search/match program using the powder diffraction file (PDF) database 1997. The composition of the metal corrosion products were determined based on the strongest reflection lines in the XRD patterns according to the PDF.[31]

RESULTS AND DISCUSSION

The marine and industrial areas studied present highly specific levels of contaminants and RH. Tables 2 and 3 present the variation in the levels of pollutants, RH, and rainfall over these sites for 12 months and average values of 1-year to 5-year exposures, respectively. Chloride was registered at the marine environment site where the levels were as high as 304.5 mg/(m²-day) and the SO_2 levels were found to be 18 mg/(m²-day) during the first year. The industrial area registered chloride concentrations of around 75 mg/(m²-day), which is lower than the concentrations found at the marine site. The SO_2 level in this site was particularly high due to the industrial nature of these areas. This site registered the fifth highest level among 41 exposure sites in India.[18] The RH levels are fairly high in both sites as compared with other studies carried out in marine and industrial areas.[18]

TABLE 4

Average Sulfur Dioxide and Chloride Deposition Rate and Atmosphere Classification Categories According to ISO/DIS 9223

	SO_2		Chloride	
Environment	Deposition Rate (mg/m^2-day)	Category	Deposition Rate (mg/m^2-day)	Category
Marine	18	P_1	304.60	S_3
Industrial	25	P_1	75.21	S_2

TABLE 5

Classification of Corrosivity Categories Corresponding to the First-Year Corrosion Rate (mm/y) of Metals According to ISO/DIS 9223

	Mild Steel		Zinc		Galvanized Iron		Aluminum	
Environment	CR	CC	CR	CC	CR	CC	CR	CC
Marine	524.00	C_5	7.10	C_5	11.66	C_5	8.6	C_5
Industrial	111.50	C_5	3.07	C_4	4.56	C_5	1.41	C_3

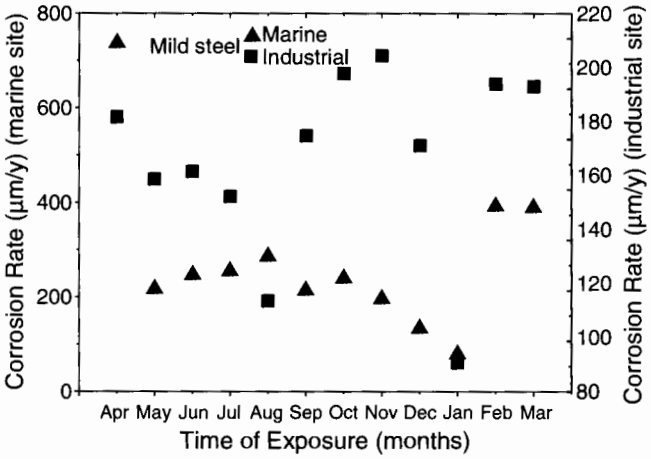

FIGURE 1. *Monthly variation of corrosion rate of mild steel exposed to marine and industrial environments, Chennai.*

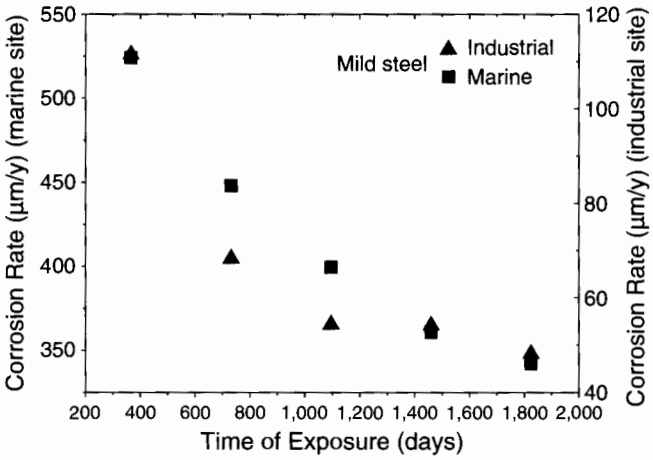

FIGURE 2. *Yearly variation of corrosion rate of mild steel exposed to marine and industrial environments, Chennai.*

Tables 4 and 5 show the environment category, the values of the corrosion rate (first year) for each of the metals studied, and the corrosiveness category determined in each case after application of the ISO 9223 norm. Using this classification, marine atmosphere was classified as S_3P_1 (300 mg/[m^2-day] to 1,500 mg/[m^2-day] Cl^- and 10 mg/[m^2-day] to 35 mg/[m^2-day] SO_2) and the industrial exposure site was classified as S_2P_1 (60 mg/[m^2-day] to 300 mg/[m^2-day] Cl^- and 10 mg/[m^2-day] to 35 mg/[m^2-day] SO_2). These two sites are considered a mixed type of atmosphere.

Mild Steel

The corrosion rate of mild steel exposed for a 1-month interval is shown as Figure 1. It was found that the corrosion rate at the marine and industrial sites varied between 79 µm/y and 737.5 µm/y, depending on seasonal variations and the corrosion rate, which was high at the marine site—about three times higher than at the industrial site. The rate was decreased in the dry season period (January through February). Mild steel behaves in different ways in the area, depending on where it is located. The yearly corrosion rate variation of mild steel panels is shown in Figure 2 as a function of exposure time. The above plot was obtained from the average values obtained from triplicate panels. The corrosion rates of mild steel found in the industrial site was lower than the marine site and the corrosiveness category was C_5 (high). An observation of the exposed mild steel panels at the industrial site revealed that the rust was powdery and uniform (brown in color), covering the entire surface within the period of one year. The product layer was highly adherent to the metal surface. The very high corrosion rate was found at the marine site and the category of corrosiveness was C_5 (very high). At the marine site, the powdery and flaky rust prod-

ucts were observed on the mild steel after 8 months of exposure (Figure 3). In general, there is correspondence between the level of pollutants and the high corrosion rates. The marine site in the port of Chennai had the highest levels of chloride, dust particles, and some quantity of SO_2 (Table 2) over the whole study and higher levels of SO_2 with lower levels of chloride at the industrial site. As far as the relative humidity (RH) is concerned, both sites had high levels. The corrosion rates observed in the sites, which are marine and industrial in nature, are similar to those obtained for highly aggressive geographic areas.[32-33] The chloride ions and the SO_2 are found to be the main factors influencing the process of corrosion with more emphasis on the chloride ion. In general, there are a large number of studies that correlate the corrosion rate of steel with the concentration of SO_2,[34-37] but few relating the same to the concentration of chloride ions. The corrosiveness category obtained according to the pollution parameters (Table 4) coincide with the data obtained using weight loss. The higher corrosion rates at the marine site may be due to the increase in electrochemical activity at the metal/rust interface in the presence of moisture, salt, and dust particles deposited on the surface. In the industrial atmosphere, almost a constant quantity of SO_2 pollutant was observed throughout the year and the fluctuation of salinity deposit was observed during the monsoon period.

In the presence of SO_2 and fog, acid precipitation occurred on the metal surface. The acid conditions combined with the marine environment and humidity result in a severe atmospheric corrosive environment (moisture accelerates the adsorption of SO_2 and thereby accelerates the formation of rust). It can also be seen from Figure 2 that the corrosion rate of mild steel decreased with exposure time at both exposure sites. In the presence of acid, the initially formed feroxyhyte (δ–FeOOH) may be converted into the protective lepidocrocite (γ–FeOOH).[38]

The plots of log corrosion data vs. log exposure time are linear. Thus, it is reasonable to accept the verification of the law of power functions (Equation [1]) to estimate long-term corrosion of mild steel, and the values of statistical parameters obtained from these plots are given in Table 6. The correlation coefficient (r^2) for the analysis is 0.97 and 0.99 for industrial and marine, respectively, which indicate an excellent correlation of the data (Table 6).

FIGURE 3. *Appearance of mild steel after 8 months' exposure at the marine site.*

At the industrial site, the "n" value indicates that the corrosion of mild steel is under the diffusion of a corrosive species, which is the rate-determining step (i.e., n = 0.5, when the current's film is protective and inhibits further corrosion by diffusion). On the other hand, "n" values >0.5 are observed at the marine site, indicating that the acceleration of the diffusion process is a result of rust detachment by erosion, diffusion, flaking, cracking, and others.

The value of k is equal to the corrosion loss after a first-year exposure and indicates the vulnerability to rusting at the beginning of the exposure. The value of "k" for industrial and marine exposure sites show a higher value of k (107.74 μm/y and 531.61 μm/y).

Table 7 shows that the main phase in the oxide layer formed on mild steel exposed at the marine site is magnetite (Fe_3O_4), hydrated maghemite (γ-$Fe_2O_3 \cdot H_2O$), ferric chloride ($FeCl_3$) with a strong reflection line at 2.51 Å, followed by lepidocrocite (3.26 Å). The strong reflection at 2.51 Å shows the formation of powdery and flake-off-type corrosion products. Misawa, et al.,[39] explained the mechanism of the formation of various types of iron oxide and iron hydroxide. The amorphous phase formed during long-term ex-

TABLE 6

Corrosion Kinetic Parameters k, n, and Correlation Coefficient r^2 for Mild Steel, Galvanized Iron, Zinc, and Aluminum

	Mild Steel			Galvanized Iron			Zinc			Aluminum		
Environment	k (μm/y)	n	r^2	k (μm/y)	n	r^2	k (μm/y)	n	r^2	k (μm/y)	n	r^2
Marine	531.61	0.79	0.99	11.36	—	0.99	7.13	1.28	0.99	8.47	1.46	0.99
Industrial	107.74	0.49	0.96	4.52	0.70	0.99	2.99	0.63	0.97	1.41	0.99	0.98

TABLE 7

X-Ray Diffraction Data for Corrosion Products of Mild Steel, Zinc, and Aluminum Exposed for One Year at Marine and Industrial Sites

	Mild Steel			Zinc			Aluminum		
Environment	d (Å)	Phase	I/Io (%)	d (Å)	Phase	I/Io (%)	d (Å)	Phase	I/Io (%)
Marine	2.51	Fe_3O_4	100	2.7	$ZnCO_3ZnCl_2$	100	3.0	$Al_2(SO_4)\cdot 4H_2O$	100
	2.9	$FeCl_3$	87	2.51	$4Zn(OH)_2$	82	4.8	$Al(OH)_3\cdot Al_2O_3\cdot H_2O$	98
	3.26	γ-FeOOH	85	1.88	ZnO	67	6.5	$Al_2O(OH)_2$	88
	6.2	$\gamma\text{-}Fe_2O_3\cdot H_2O$	82	26.4	$ZnCl_2$ ZnS	67			
					$4ZnO\cdot CO_2\cdot 4H_2O$		3.1	$Al_2(SO_4)\cdot 4H_2O$	100
Industrial	2.43	$Fe(OH)_2$	100				3.5	$Al(SO_4)_3$	96
	1.56	FeO, Fe_3O_4,	88	2.96	$3Zn(OH)_2\cdot NaCl\cdot 6H_2O$	63	7.0	$Al_2SO_4\cdot 5H_2O$	83
	1.49	FeS	87	4.13	$ZnSO_4$	49			
		$\gamma\text{-}Fe_2O_3$							

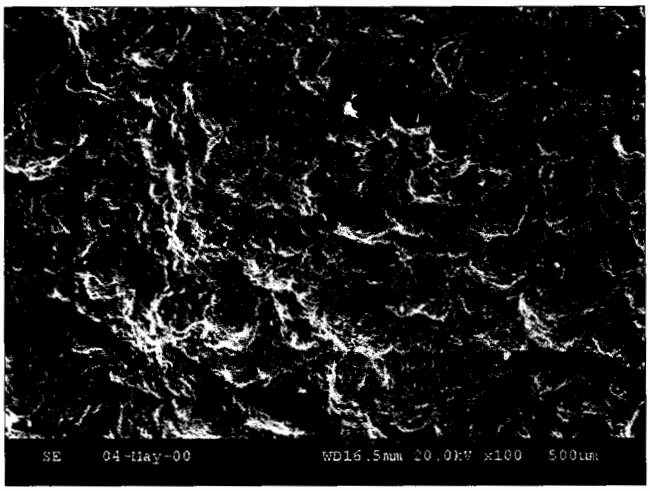

FIGURE 4. *SEM structure of the rust surface of mild steel exposed for one year at the marine site.*

posure on steel acted as a protective barrier against atmospheric corrosion. SEM (Figure 4) investigation revealed that corrosion losses are mainly due to the flake off of particles from the rust layer. Table 7 gives the composition of corrosion products obtained from the XRD method for mild steel exposed at industrial environment. A similar result was obtained for mild steel in the industrial environment compared with the XRD results obtained in the marine environment. α-FeO(OH) (geothite), $Fe(OH)_2$ (2.43 Å) (ferrous hydroxide) $\gamma\text{-}Fe_2O_3\cdot H_2O$ (6.15 Å) (hydrated maghemite), $FeCl_2\cdot 2H_2O$ (2.57 Å) (hydrated ferrous chloride), FeS (ferrous sulfide), and Fe_3O_4 (1.56 Å) (magnetite) were the main corrosion products observed at the industrial exposure site.

Galvanized Iron and Zinc

The monthly corrosion rate of GI in the marine and industrial sites varied between 0.82 μm/y and 58.1 μm/y and 1.1 μm/y and 49.6 μm/y (Figure 5), respectively. The corrosion rate was much higher at both exposure sites during June and July. In the case of zinc (Figure 6), the corrosion rate in the industrial atmosphere varied between 3.4 μm/y and 154 μm/y and the rates at the marine site were more or less the same as in the industrial site. The corrosion rate of zinc was very high during the southwest monsoon periods. In these periods, the wind velocity and RH were also very high at both exposure sites.

Figures 7 and 8 illustrate the yearly corrosion rates of GI and zinc as a function of exposure time, respectively. The corrosiveness categories of GI and zinc in the marine site were C_5 and C_5, and in the industrial site, they were C_4 and C_5, respectively. The yearly corrosion rate of GI and zinc (Figure 6) was very high in the marine environment compared with the industrial environment. The first-year corrosion rate of GI was found to be 11.66 μm/y and 4.56 μm/y at the marine and industrial environments, respectively. At the end of the second-year exposure, it was observed that all the zinc coatings were removed from the entire base metal surface at the marine site. This may be due to the formation of a galvanic cell and the ability of zinc coatings to provide sacrificial protection to the steel substrates where it is exposed to high salinity content in the atmosphere (RH > 70%) at pores, scratches, and cut edges, which is an important feature. The exposed zinc surface is characterized by the loss of the shiny appearance and the white rust formation on it, which was more noticeable on the sample exposed in the marine site. It can be observed that the corrosion rate of zinc increased significantly with high atmospheric chloride pollution, so that the zinc corrosion shows a linear behavior.[40-42] However, the SO_2 content of the marine atmosphere is also a significant factor in the atmospheric corrosion of zinc. Other atmospheric parameters such as RH, rain fall, pollutants other than chloride and SO_2, and soil particles deposition also seem to be important. In Figure 6, the zinc corrosion decreased with time at the industrial site, and the corrosion did not show linear behavior.[40-43] The corrosion rate of zinc was found to be about 63% lower than that of GI in the marine atmosphere whereas in the industrial atmosphere,

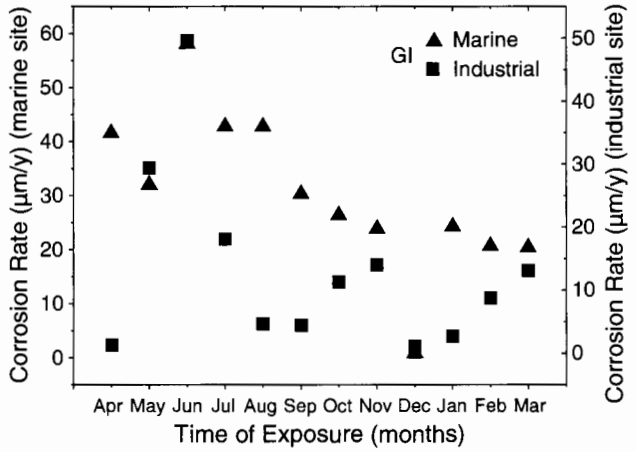

FIGURE 5. *Monthly variation of corrosion rate of GI exposed to marine and industrial environments, Chennai.*

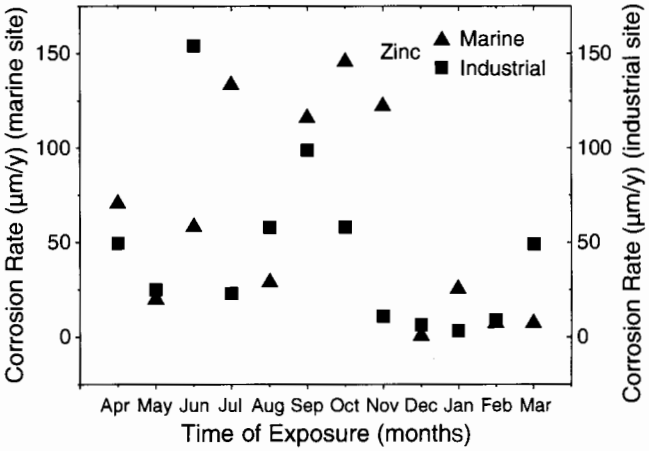

FIGURE 6. *Monthly variation of corrosion rate of zinc exposed to marine and industrial environments, Chennai.*

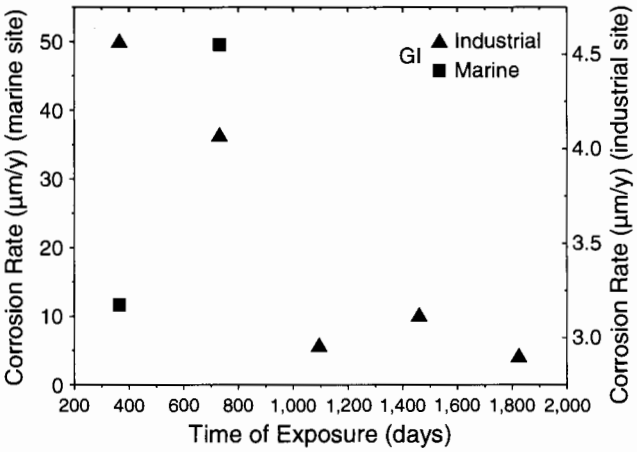

FIGURE 7. *Yearly variation of corrosion rate of GI exposed to marine and industrial environments, Chennai.*

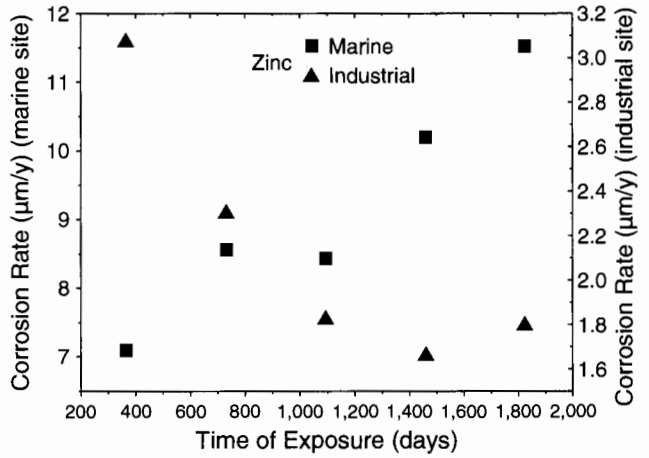

FIGURE 8. *Yearly variation of corrosion rate of zinc exposed to marine and industrial environments, Chennai.*

the corrosion rate of zinc was found to be about 45% lower than GI. The visual observations of zinc metal exposed for one year indicated that at the marine site, the corrosion product density was much greater than at the industrial site. At the two exposure sites, very high corrosion loss was observed. The value of "n" was close to 0.5 for GI exposure at the two sites, indicating a diffusion-controlled mechanism. The combined influence of n and k leads to initially higher corrosion loss with film formation.

In the case of zinc, the "n" value is similar to GI in the industrial exposure site, and in the marine site, the value of "n" is >1, indicating that mixed diffusion and charge-transfer control and a gradual change from diffusion control to charge-transfer control due to the presence of protective film corrosion products layer on the metal surface, on the surface that was either bare or not covered with layers, reduce diffusion of corrosion species to the metal surface.

Table 7 shows the XRD pattern for the corrosion of zinc in the marine environment. The corrosion products formed during the first year of exposure included zinc carbonate ($ZnCO_3$), simonkolleite ($Zn_5[OH]_8Cl_2H_2O$), basic zinc chloride ($ZnCl_2.4Zn[OH]_2$), followed by zinc sulfide (ZnS), zinc oxide (ZnO), and zinc sulfate ($ZnSO_4$), which are commonly found on zinc exposed to atmospheres with a high saline content. In the marine site, the higher corrosion rates of zinc may be due to the formation of simonkolleite ($Zn_5[OH]_8Cl_2H_2O$) and basic zinc chloride,[43] and this compound possessed high solubility and can dissolve in weak acid solutions such as rainfall or dew. But, in the industrial atmosphere, inhibition of the corrosion of zinc was observed, which may be due to the formation of sodium zinc hydroxychloride sulfate ($ZnSO_4 \cdot 3Zn[OH]_2 \cdot NaCl \cdot 6H_2O$)[44] on the zinc metal surface. This compound is responsible for the inhibition of the corrosion of zinc in mixed environments.

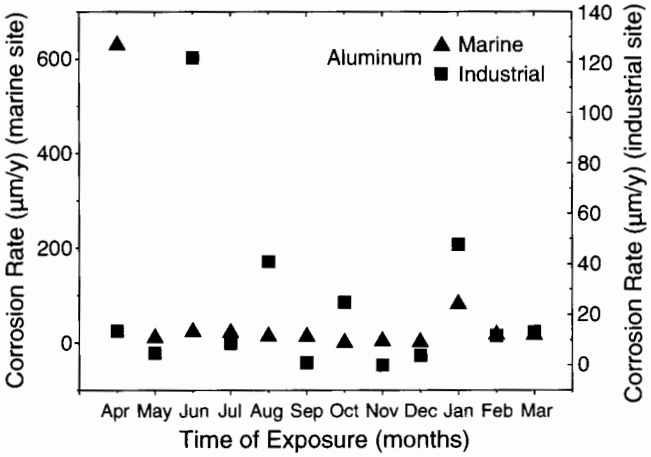

FIGURE 9. *Monthly variation of corrosion rate of aluminum exposed to marine and industrial environments, Chennai.*

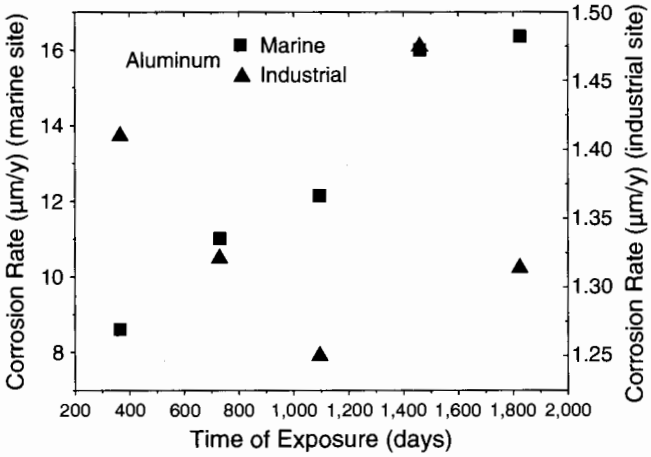

FIGURE 10. *Yearly variation of corrosion rate of aluminum exposed to marine and industrial environments, Chennai.*

Aluminum

For aluminum, monthly variation of the corrosion rate was low at both exposure sites in comparison with other metals. The seasonal variation of the corrosion rate of aluminum was mainly dependent on salinity, SO_2, and RH content in the atmosphere. The corrosion rates found for aluminum (Figure 9) in the marine exposure site were considerably greater than the industrial exposure sites. Aluminum corrosion in the marine atmosphere depends on salt deposited on the metal surface. The salinity seems to be very highly aggressive to aluminum in the marine site compared to the industrial site. Pitting corrosion observed within the period of one year in the marine atmosphere is considerably more pronounced than in the industrial atmosphere. In the marine atmosphere, the corrosion rate of aluminum increased with exposure time (Figure 10). The attack for aluminum in this environment increased very quickly with exposure time, in agreement with severe pitting and continuous soluble corrosion products that form on the metal surface with increased exposure time. In the case of the industrial exposure site, the corrosion rate decreased with the exposure time. The attack for aluminum in this type of atmosphere decreased very quickly with exposure time, as a result of the formation of the thick and continuous corrosion product layers on the metal surface. Vilche, et al.,[45] demonstrated that in the case of aluminum, the corrosion product layer, which consisted of aluminum oxides, covered the surface of the aluminum and protected it by preventing moisture penetration.

The graphically determined n, k, and r^2, thus obtained, are given in Table 6 for aluminum. The value "n" for both sites indicates the gradual change from diffusion control to a charge-transfer control mechanism. The main composition of the corrosion products are (Table 7) hydrated aluminum sulfate ($Al_2SO_4 \cdot H_2O$) at a strong reflection line of 3.07 Å followed by aluminum hydroxide ($Al[OH]_3$), hydrated aluminum oxide ($Al_2O_3 \cdot H_2O$), and aluminum oxyhydroxide ($Al_2O[OH]_2$). Macroscopically severe superfacial pitting corrosion attack was observed at the marine site.

Comparison of Results of Four Metals

The average corrosion rates of metals in the marine site were generally larger than those of the industrial site. The average first-year corrosion rates of the metals were in the order of mild steel (319.5 μm/y) > GI (60.8 μm/y) > zinc (15.45 μm/y) > and aluminum (5.0 μm/y). In particular, the corrosion rate of mild steel was remarkably greater than the other test metals, which was estimated to be about 5 to 64 times larger than those for GI, zinc, or aluminum. Corrosion rates of 27.42 μm/y to 1,600 μm/y were reported for the average marine corrosion rate of mild steel during the first year, and 16 μm/y to 300 μm/y for the average industrial corrosion rate of mild steel.[18] In our study, the average corrosion rate of mild steel was 524 μm/y and 115 μm/y in marine and industrial sites, respectively, which show lower corrosion rates.

CONCLUSIONS

❖ Monthly variation and yearly corrosion rates of mild steel, zinc, GI, and aluminum were higher at the marine site than at the industrial site. This may due to the higher chloride content at the marine site. At both environmental sites, a linear law of corrosion loss with exposure was observed. The main products found in the oxide layer of the mild steel were magnetite and lepidocrocite at the marine and industrial environments. The oxide layer was more of the flake-off type on the mild steel exposed at the marine site than for industrial site, suggesting higher aggressiveness at the marine site. Regression analysis was made to fit the experimental data obtained with the four metals

tested at the industrial and marine atmospheres in Chennai. A very high correlation coefficient r^2 was found in all the cases. Simonkolleite ($Zn_5[OH]_8Cl_2H_2O$) and basic zinc chloride were formed on the zinc surface in the marine atmosphere, which is soluble in rain water or dew, and hence, the zinc corrosion showed a linear behavior in this atmosphere. In the industrial atmosphere, inhibition of the corrosion of zinc was observed due to the formation of $ZnSO_4 \cdot 3Zn(OH)_2 \cdot NaCl \cdot 6H_2O$. This insoluble compound is responsible for the inhibition of the corrosion of zinc in mixed environments.

❖ At the marine site, it was seen that at the end of the second year, the zinc coatings on the GI surface was removed. This may be due to the formation of a galvanic cell and the ability of zinc coatings to provide sacrificial protection to the steel substrates. The study of galvanized steel in the industrial site established that during the atmospheric corrosion process, a complex layer composed of a thin and compact ZnO inner layer and a thick and porous $2ZnCO_3 \cdot 3Zn(OH)_2$ outer layer decreased the corrosion rate with time. This surface film seems to inhibit further metal dissolution, although the environmental conditions determine the extent of corrosion progress, as there is a competition between film removal and film formation reactions. The attack of aluminum in the marine environment increased with exposure time because of the severe pitting and formation of soluble corrosion products of aluminum. In the case of the industrial exposure site, the corrosion rate decreased with exposure time, due to the formation of thick and continuous corrosion product layers. The corrosion product layers on aluminum protected it by preventing the ingress of moisture and corrosive ions.

REFERENCES

1. S. Jouen, B. Hannoyer, A. Barbier, J. Kasperek, M. Jean, Mater. Chem. Phys. 85 (2005): p. 75.
2. M. Morcillo, B. Chico, D. de la Fuente, E. Almeida, G. Joseph, S. Rivero, B. Rosales, Cold Reg. Sci. Technol. 40 (2004): p. 165.
3. S. Qesch, P. Heimgartner, Mater. Corros. 47 (1996): p. 425.
4. A. Abdul Wahab, Pract. Period. Hazard. Toxic Radioact. Waste Manage. 8 (2004): p. 274.
5. H.E. Townsend, A.R. Borzillo, Mater. Perform. 26, 7 (1987): p. 37.
6. F.W. Lipfert, Mater. Perform. 26, 7 (1987): p. 12.
7. F.H. Haynie, J.B. Upham, Mater. Perform. 9 (1970): p. 35.
8. R. Eriseson, Werkst. Korros. 29 (1978): p. 400.
9. L.R. Walton, J.B. Johnson, G.C. Wood, Br. Corros. J. 17 (1982): p. 65.
10. J.E. Svensson, L.G. Johansson, Corros. Sci. 34 (1993): p. 721.
11. P. Eriksson, L.G. Johansson, J. Gullmann, Corros. Sci. 34 (1993): p. 1,083.
12. S.W. Dean, W.H. Anthony, ASTM STP 965, "Degradation of Metals in the Atmosphere" (West Conshohocken, PA: ASTM International, 1986), p. 191.
13. K. Barton, E. Beranek, Werkst. Korros. 6 (1959): p. 377.
14. S. Oesch, P. Heimgariner, Mater. Corros. 47 (1996): p. 425.
15. R. Bhaskaran, N. Palaniswamy, N.S. Rengaswamy, M. Jayachandran, "Global Cost of Corrosion: A Historical Review," in ASM Handbook, vol. 13B (Materials Park, OH: ASM International, 2005), p. 619.
16. M. Natesan, N. Palaniswamy, N.S. Rengaswamy, S. Rajesh Kumar, M. Raghavan, "Corrosion Map—A Global Perspective," Proc. 7th Int. Symp. on Advances in Electrochemical Science and Technology (ISAEST VII), held Nov. 2002 (Karaikudi, India: The Society for Advancement of Science and Technology, 2002), p. 52.
17. M. Natesan, N. Palaniswamy, N.S. Rengaswamy, Mater. Perform. 45, 1 (2006): p. 52.
18. M. Natesan, G. Venkatachari, N. Palaniswamy, Corros. Prev. Control 52, 2 (2005): p. 43.
19. P. Rajendran, "Investigation on Atmospheric Corrosion of Metals in Industrial Environment and Their Protection" (Ph.D. thesis, Bharathiar University, Coimbatore, T.N. India, 1995).
20. P.S. Mohan, M. Natesan, M. Sundaram, K. Balakrishnan, Bull. Electrochem. 12 (1996): p. 91.
21. ISO 8565, "Metals and Alloys. Atmospheric Corrosion Testing, General Requirements for Field Test" (Geneva, Switzerland: International Organization for Standardization [ISO], 1992).
22. ISO 5555-1970, "Code of Practice for Conducting Field Studies on Atmospheric Corrosion of Metals," Indian Standard (Geneva, Switzerland: International Organization for Standardization [ISO], 1970).
23. ASTM G 90, "Standard Practice for Preparing, Cleaning, and Evaluating Corrosion Test Specimens (West Conshohocken, PA: ASTM International, 1990).
24. ASTM G 50-76 (reapproved 1997), "Standard Practice for Conducting Atmospheric Corrosion Testing Metals" (West Conshohocken, PA: ASTM International, 1997).
25. ASTM D 2010-85, "Standard Method for Evaluation of Total Sulfation Activity in the Atmospheric by Lead Dioxide Candle" (West Conshohocken, PA: ASTM International, 1985).
26. ISO/DIS 9223, "Corrosion of Metals and Alloys—Classification of Corrosivity of Atmospheres" (Geneva, Switzerland: International Organization for Standardization [ISO], 1992).
27. M. Pourbaix, "The Linear Bilogarithmic Law for Atmospheric Corrosion," in Atmospheric Corrosion, ed. W.H. Ailor (New York, NY: John Wiley, 1982), p. 107.
28. ASTM G 16-95 (reapproved 1999), "Standard Guide for Applying Statistics to Analysis of Corrosion Data" (West Conshohocken, PA: ASTM International, 1999).
29. ASTM G 101-01, "Standard Guide for Estimating the Atmospheric Corrosion Resistance of Low-Alloy Steels (West Conshohocken, PA: ASTM International, 2001).
30. J.J. Santana Rodriguez, F.J. Santana Hernandez, J.E. Gonzalez Corros. Sci. 45 (2003): p. 799.
31. JCPDS, X-Ray Diffraction Data Cards of the Joint Committee on Powder Diffraction Standards (International Center for Diffraction Data, 1997).
32. S.-T. Kim, Y. Macda, Y. Tsujino, Atmos. Environ. 38 (2004): p. 37.
33. Z. Ahmad, J.M. Allam, B.J. AbdulAleem, Anti-Corros. Methods Mater. 47, 4 (2000): p. 215-223.
34. F. Mansfeld, ed., Corrosion Mechanisms (New York, NY: Marcel Dekker, 1987), p. 241.
35. J.C. Hudson, J.F. Stanners, Appl. Chem. 3 (1953): p. 186.
36. K. Barton, E. Beranez, G.V. Akimov, Werkst. Korros. 6 (1959): p. 337.
37. T. Sydberger, N.G. Vannerberg, Corros. Sci. 12 (1972): p. 775.
38. H. Okada, Y. Hosoi, H. Naito, "The Protective Rust Layer Formed on Low-Alloy Steel in Atmospheric Corrosion," 4th Int. Cong. Met. Corros., Extended Abstracts (Houston, TX: NACE, 1969), p. 96.
39. T. Misawa, K. Hashmoto, S. Shimodaira, Corros. Sci. 14 (1974): p. 131.
40. T.E. Graedel, J. Electrochem. Soc. 136, 4 (1989): p. 193C-203C.
41. M.E.M. Almeida, M.G.S. Ferreira, Atmospheric Corrosion Maps of Portugal (Lisbon, Portugal: INETI, 1997), p. 341-344.
42. R.A. Legault, "Atmospheric Corrosion of Galvanized Steel," offprint from Atmospheric Corrosion, ed. W. Ailn (1982), p. 607-613.
43. E. Almeida, M. Morcillo, B. Rosales, Br. Corros. J. 35 (2000): p. 289.
44. J.M. Costa, M. Vilarrasa, Br. Corros. J. 28 (1993): p. 117.
45. J.R. Vilche, E.E. Varela, G. Acura, E.N. Codaro, B.M. Rosales, A. Fernandez, G. Moriena, Corros. Sci. 37, 6 (1995): p. 941.